Proceedings of the 12th International Conference on Quasicrystals (ICQ12)

Inverse Hall–Petch Like Mechanical Behaviour in Nanophase Al–Cu–Fe Quasicrystals: A New Phenomenon

N.K. Mukhopadhyay[a,*], F. Ali[b], S. Scudino[c], M. Samadi Khoshkhoo[c], M. Stoica[c], V.C. Srivastava[d], V. Uhlenwinkel[e], G. Vaughan[f], C. Suryanarayana[g] and J. Eckert[c,h]

[a]Department of Metallurgical Engineering, Indian Institute of Technology (BHU), Varanasi 221 005, India

[b]Pakistan Institute of Engineering & Applied Science, P.O. Nilore, Islamabad, Pakistan

[c]IFW Dresden, Institut für Komplexe Materialien, Postfach 27 01 16, D-01171 Dresden, Germany

[d]Metal Extraction & Forming Division, National Metallurgical Laboratory, Jamshedpur-831007, India

[e]Institut für Werkstofftechnik, Universität Bremen, Badgasteiner Str. 3, D-28359 Bremen, Germany

[f]European Synchrotron Radiation Facilities ESRF, BP 220, 38043 Grenoble, France

[g]Dept. of Mechanical and Aerospace Engineering, University of Central Florida, Orlando, FL. 32816-2450, U.S.A.

[h]TU Dresden, Institut für Werkstoffwissenschaft, D-01062 Dresden, Germany

The structural and mechanical stability of quasicrystals are important issues due to their potential for possible applications at high temperatures and stresses. The aim of the present work is, therefore, to review the earlier works on conventional crystalline and quasicrystalline materials and also to report the results and the analysis on the Hall–Petch and inverse Hall–Petch like behavior of nanoquasicrystalline $Al_{62.5}Cu_{25}Fe_{12.5}$ alloys. It was observed that, at large grain sizes, the hardness increases with decreasing grain size, exhibiting the conventional Hall–Petch relationship, whereas for smaller grains, inverse Hall–Petch behavior was identified. The inverse Hall–Petch behavior in the nanoquasicrystalline phase could be attributed to thermally activated shearing of the grain boundaries, leading to grain boundary sliding in nanostructures of quasicrystalline grains. These results were analyzed based on the dislocation pile-up model as well as the grain boundary shearing models applicable to nanomaterials.

DOI: 10.12693/APhysPolA.126.543

PACS: 61.44.Br

1. Introduction

Strengthening of ductile materials as well as softening of brittle materials is a well-known strategy for improving materials performance by grain refinement from micro- to nanoscale. For conventional polycrystalline metallic alloys, the general relationship between yield stress and grain size (crystallite size),which was earlier advocated by Hall [1] and extended by Petch [2], is known as Hall–Petch (HP) relationship, providing a semi-empirical guideline to grain size dependent strength, and can be expressed [1–5] as

$$\sigma = \sigma_0 + kd^{-\frac{1}{2}}, \tag{1}$$

where σ_0 is the frictional stress representing the overall resistance of crystal lattice to dislocation movement, k is the locking parameter which measures the relative hardening contribution of the grain boundaries and d is the average diameter of the grains representing the crystallite size. A similar expression can be provided for the hardness as

$$H = H_0 + k_H d^{-\frac{1}{2}}. \tag{2}$$

It is understood, based on the original dislocation pile-up model for HP relationship that the grain boundaries act as barriers to the dislocation motion as they prevent movement of dislocations from one grain to another. As a result, it leads to the pile-up of dislocations giving rise to the strengthening effect.

However, it is intuitive that the HP relation cannot be extrapolated to the smallest grain size as the dislocation behavior and their interaction with grain boundaries may be different depending on the grain sizes. In fact, the dislocation activity as observed in microscale grained materials will be completely different in nanoscale grained materials, as being reported in the literature. Therefore, Eqs. 1 and 2 may not be valid for nanoscale grains and the materials may get softened rather than hardened due to the absence of dislocation pile-up mechanisms.

The grain size softening at nanoscale level is in general known as inverse Hall–Petch (IHP) behavior [5–11]. This idea has been shown to work in brittle ceramics for enhancing their toughness and ductility [12]. It may be emphasized that though the HP behavior is somewhat understood in metallic alloys, the IHP behavior at nanoscale is yet to be understood properly. There are various schools of thought to interpret these effects.

According to one school, the IHP behavior observed in materials can be considered to be the result of artifact because the materials processed by two steps, i.e., powder processing followed by compaction and sintering, leads to alterations in the pore size and distribution and

*corresponding author; e-mail: mukho.met@iitbhu.ac.in

other defects which in turn cause this apparent effect of softening. Thus, it is cautioned that the processing of material is an important issue while interpreting the IHP behavior. Normally, IHP behavior is reported for grain sizes in the range of 10-30 nm, for pure metals and crystalline intermetallics [3, 13–25]. Though most of the attempts are directed to understand the IHP behavior using the concept of grain boundary sliding, there are reports attributing to dislocation mobility in the grain boundaries to account for this effect [17]. The existence of free volume present in the nanocrystalline materials has also been shown to explain this effect [26].

It is now well understood that quasicrystals (QCs), a special class of complex metallic alloys, display peculiar structures exhibiting translational aperiodicity as well as non-crystallographic rotational symmetries [27–30]. Due to the presence of dislocation-like defects, which are immobile due to aperiodicity, and absence of proper slip planes like in crystalline alloys, quasicrystalline materials become hard, brittle and are strain softened.

However, dislocation mediated materials flow and deformation is observed at moderate to high temperatures [31], implying that enough thermal energy is available to overcome the activation barrier for deformation mainly through dislocation climb. The limited deformation of quasicrystals, at low temperature, is observed to take place by shear band formation, implying the localized shearing among atoms, under stress rather than dislocation movement [5, 32–35]. This behavior is very similar to the deformation of metallic glasses [36]. It is argued that phason strain, which causes phason disordering in the quasicrystalline materials during deformation, increases when the stress is applied. After a critical value, the localized shearing causes permanent deformation leading to the formation of shear bands. Further increase in strain may cause phase transformation to a crystalline phase or microcracking [5, 37–39]. As quasicrystalline materials are hard and brittle, there are attempts to synthesize the nanocrystalline materials by using mechanical milling/alloying techniques. Thus, the deformation and indentation behavior of quasicrystals of various crystallite sizes is an important issue. In spite of the structural complications, the HP and IHP behaviors have been reported in Al-Fe-Cu icosahedral quasicrystals [29, 40].

The aim of the present work is to review the earlier work and discuss some of our results in the context of HP and IHP behaviors in nano-crystalline and nanoquasicrystalline materials. The detailed investigation along with the analysis, based on the current understanding in the context of deformation of nanocrystalline and nanoquasicrystalline alloys, will be presented.

2. Experimental details

The quasicrystalline material with the nominal composition of $Al_{62.5}Cu_{25}Fe_{12.5}$ (at.%) was produced by spray deposition (for details on sample preparation, see [41]). Mechanical milling experiments were performed using a Retsch PM400 planetary ball mill using hardened steel balls and vials with a ball-to-powder mass ratio of 10:1. Milling was conducted up to 80 h at a milling speed of 100 rpm. This low milling intensity was chosen to avoid any phase transformations, which were observed to occur at higher milling intensities [42, 43]. Mechanical milling was carried out in a controlled manner so as to avoid any phase transformation but to allow the formation of nano QC phases. To avoid or to minimize possible atmospheric contamination during milling, all sample handling was carried out in a glove box under purified argon atmosphere (less than 1 ppm O_2 and H_2O). No process controlling agent was used. Detailed X-ray diffraction (XRD) analysis was carried out using conventional X-rays (Co-K_α) as well as a high-energy monochromatic synchrotron beam ($\lambda = 0.011249$ nm) at the ID11 beamline of the European Synchrotron Radiation Facilities (ESRF). Electron microscopy was carried out to investigate the grain sizes using a Philips CM-20 and FEI: Tecnai $20G^2$ electron microscopes operating at 200 kV, and to ascertain if any other phases have formed. The milled powders were embedded in epoxy resin (Struers Specific-20, room temperature curing) and polished for microhardness measurements. The Vickers microhardness tests were performed using a computer-controlled Shimadzu HMV-2000 hardness tester with an applied load of 5 g and a dwell time of 10 s. The diagonal of the indentations as well as the hardness were evaluated using a Digital Video measuring system. It was ensured that the selected areas of indentation were away from the edges.

3. Results and discussion

Figure 1a shows the optical micrograph of the unmilled spray-deposited samples showing the icosahedral phase. Annealing twins, probably growth twins are seen in the larger grains. The reason for the observed twins is yet to be ascertained. Electron micrographs of these samples clearly show grains and sharp grain boundaries and no other phases (Fig. 1b). These spray-deposited materials were used for milling experiments. The hardness of this material has been observed to be 9.6 GPa. The sample did not show any cracking because of the low loads. However, at higher load of 100 g, the sample cracked (Palmqvist type) along the diagonal. The fracture toughness of the sample, using the appropriate model, has been found out to be 1.2 MPa $m^{1/2}$ [41].

The structural evolution of the spray-deposited powders as a function of the milling time during mechanical milling is presented in Fig. 2. For the sake of clarity, only selected XRD patterns are displayed in this figure. All XRD patterns of the as-prepared as well as milled samples are characterized by several distinct diffraction peaks. All these peaks were unambiguously indexed as due to the face centered icosahedral (FCI) quasicrystalline phase. The superlattice peak (311111), indicating FCI ordering [44], can be seen distinctly.

It is interesting to note that the peaks corresponding to superlattice peaks (311111) survived till 80 h of milling implying that milling has not destroyed the structural

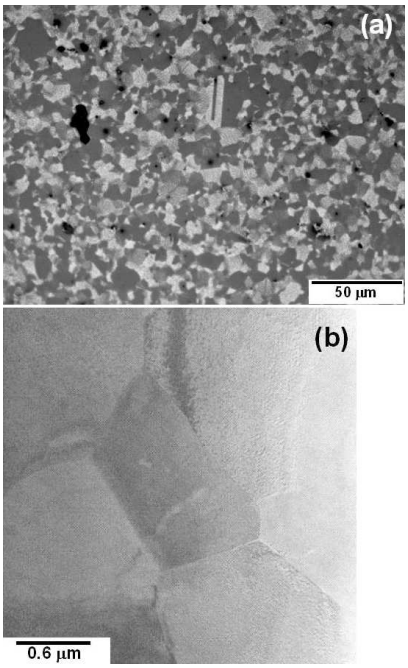

Fig. 1. (a) Optical microscopy image showing the grains of the QC phase in as-sprayed deposited material. The annealing twin like features can also be observed in the relatively bigger grains. (b) Electron microscopy image of the as-deposited material (bright field) showing the grains and their sharp grain boundaries.

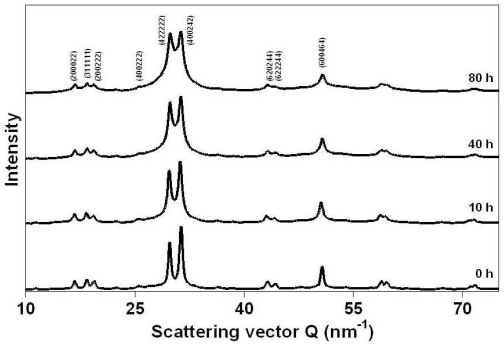

Fig. 2. Synchrotron X-ray diffraction patterns (λ = 0.01129 nm) of the as-deposited and mechanically milled $Al_{62.5}Cu_{25}Fe_{12.5}$ quasicrystals, showing the gradual change of the diffraction peaks signifying the reduction of crystallite sizes as well as increase of lattice strain.

ordering, even though phason disordering is inevitable during milling. There are attempts to ascertain the degree of order with respect to milling. It is found in the present case that, at the initial stages of milling, the order parameter increases and then decreases; but does not reach the zero value. The effect of milling on chemical ordering will be discussed elsewhere.

It is clear that no additional diffraction peaks are observed, implying that no phase transformation had occurred under these experimental conditions. However, there is a noticeable broadening of the diffraction peaks, which increases with the milling time. This indicates that a decrease of grain size and increase of lattice strain occur during milling. Figure 3a–c shows the electron diffraction pattern, dark-field and bright-field images, respectively, from the 40 h milled sample. Extensive electron microscopy was carried out to determine the average grain size from the dark-field images.

TABLE

The milling time and corresponding grain size and hardness have been displayed for $Al_{62.5}Cu_{25}Fe_{12.5}$ icosahedral quasicrystals.

Milling time [h]	Grain size [nm]	Hardness [GPa]
0	2000	9.60 ± 0.5
1	88	9.76 ± 0.5
5	48	10.70 ± 0.5
10	39	11.42 ± 0.7
20	24	10.46 ± 0.7
40	21	9.32 ± 0.8
80	18	8.57 ± 0.8

Detailed grain size reduction with milling time is seen in Fig. 4 as well as in Table. After milling for 40 h, the grain has reached around 20 nm. From Fig. 4 it appears that the grain size has reached the saturation value, after which it becomes difficult to achieve any further reduction. In fact, it has been observed that prolonged milling beyond 100 h with or without higher milling intensity, gives rise to the phase transformation to a crystalline bcc phase (i.e. completely or partially disordered B2 phase) besides the reduction of grain size and increase of lattice strain [42, 43].

The Vickers indentation experiments are carried out carefully on the mounted samples (Fig. 5). Figure 4 shows the variation of hardness and grain size with milling time. The hardness (9.6 GPa) of the initial sample (as-deposited without milling) increases with milling time in two stages, i.e., to 9.8 GPa and then to 11.5 GPa. After reaching to the maximum value of hardness of 11.5 GPa, the hardness decreases with grain size and reaches the minimum value of 8.6 GPa. The cross-over of hardness with grain size has been reported by us earlier [40]. It has also been shown that the magnitude of HP slope ($\approx$30 GPa/nm$^{1/2}$) in both the stages of HP and IHP to be nearly similar, even though it is positive in the HP regime and negative in the IHP regime [40]. There is no specific interpretation of this phenomenon, suggesting that it requires further study.

Figure 6 shows the data from nano-QC Al-Fe-Cu alloys (present study) and nano-Zn [21] samples. In order to better appreciate the nature of HP and IHP behaviors, the normalized hardness data (i.e, H/H_{initial}) has been plotted against $d^{-1/2}$ instead of the absolute hardness values. From this figure the nature of the HP plot as

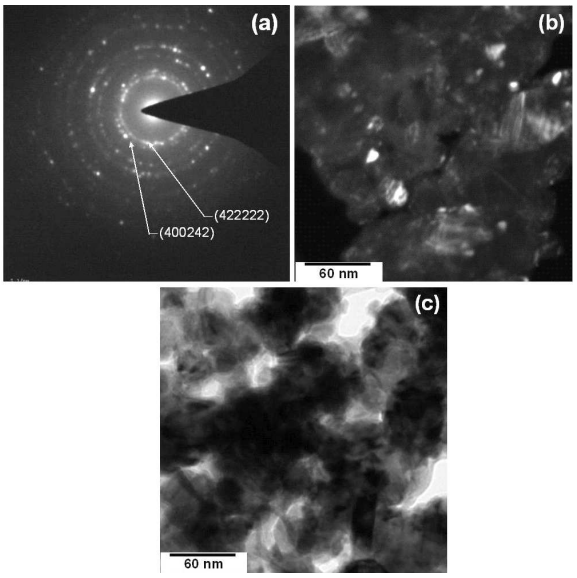

Fig. 3. (a) Electron diffraction pattern and electron microscopy images of the milled powders showing (b) dark field and (c) bright field images. The fine grain size in the order of nanometers can be seen in the dark field image of 80 h milled powder.

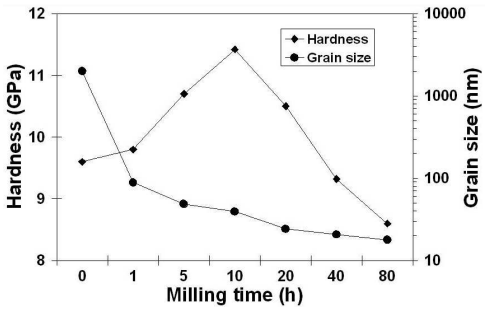

Fig. 4. Variation of hardness and grain size of QC with milling time. It is clear that initially the hardness increases and then decreases, showing the softening behavior at around 40 nm grain size. Whereas, the grain size reduces at higher rate at the initial stage and then decreases slowly.

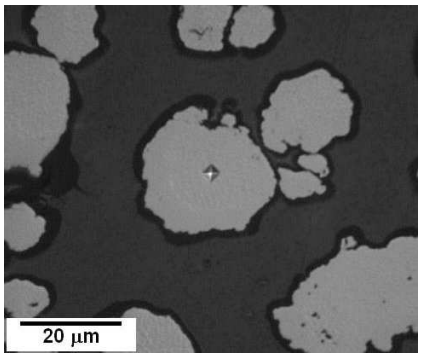

Fig. 5. The optical microscopy image showing the indentation on the milled powder of 40 h sample.

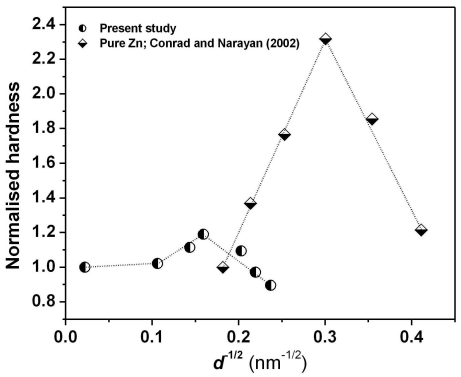

Fig. 6. Normalized hardness (H/H_{initial}) versus $d^{-1/2}$ plotted in order to understand the typical nature of HP and IHP behavior for the present nanoquasicrystalline and nano-metallic materials obtained from literature. The cross-over is clear but the relative change of hardness is less compared to Zn nanocrystals; the critical grain size is higher in case of nano-QC material.

well as the threshold grain sizes can be observed and compared between these two materials. Compared to Zn nanocrystals, the relative change of hardness for n-QC is less, but the critical grain size is larger for the nanoquasicrystalline sample.

The critical grain size has been reported for intermetallics to be in the range of 30-60 nm. For example, in case of $Nb_{77}Al_{23}$ and $NbAl_3$, it is 35 nm and 63 nm, respectively [20]. Similarly, Conrad and Narayan [20] have reported the critical grain size values for HP to IHP transition as 7 nm and 8 nm for Cu and Ni-P, respectively. In addition, computer simulated values for the critical grain size for Cu and Ni are 8 and 11 nm, respectively [20]. Hence, it is not surprising to have a large critical size value (i.e., ≈ 40 nm) for nano-QC materials.

In most metallic nanocrystalline alloys, the IHP behavior is more pronounced for grain sizes below about 10 nm. However, Chang and Chang [13] demonstrated the variation of hardness of pure Cu processed by different routes such as electroless deposited, electroplating, sputtering and bulk samples. They showed a decrease in hardness from 1.96 to 1.12 GPa for a decrease in grain size from 25 to 10 nm for electroless deposited Cu. Whereas, a decrease in grain size from 501 to 140 nm for sputtered Cu and from 4.53 μm to 43 nm for electroplated Cu led to an increase in hardness from 1.63 to 1.89 GPa and 1.29 to 2.26 GPa, respectively. This indicates a cross-over behavior for the hardness at 43 nm, when the hardness is considered without taking into account the processing route. This anomalous result may be attributed to the different processing routes utilized and the artifacts that might be generated therein.

The prediction of 10 nm or less for the critical grain size closely matches with the dislocation pile-up model [40, 45]. However, this model does not predict the correct value for the nano-QC material [40]. This

has been interpreted on the basis that dislocations are not normally mobile at room temperature in QC materials. Therefore, the dislocation pile-up model is not applicable for the prediction of strength enhancement in case of QC materials. This fact could be attributed to the complexities of the structures leading to different deformation mechanisms. Hence, it is reasonable to propose that the critical grain size be scaled with the structural complexity, i.e., it increases in the order: metals $\rightarrow$ intermetallics $\rightarrow$ QC.

It may be emphasized that the grain boundary area in nanocrystalline/quasicrystalline phases consists of a significant fraction of atoms, and consequently, these are highly disordered in nature and resemble the amorphous phase. In the absence of dislocation activity, the grain boundaries play an important role in deformation causing easy grain boundary movement. This movement has been suggested by Conrad and Narayan [20–22] to take place by the thermally activated shearing process. Following this approach, they have shown that this model is able to predict the activation energy during deformation. This approach was also adopted by Mukhopadhyay et al. [40] in order to account for the observation of IHP behavior in nanoquasicrystals.

It appears that the thermally activated shear mechanism can reasonably explain the observed features and can predict the activation energy which appears to match closely with the activation energy of grain boundary diffusion. However, in the absence of any experimental data of grain boundary diffusion of quasicrystalline phases, it can only be taken as a reasonable interpretation that grain boundary shearing event of atoms can lead to softening phenomenon in nano-QC phases.

However, the detailed mechanism of IHP behavior in the nanoscale structure is yet to be established by high resolution electron microscopy observations of the deformed region. The computer simulation model suggests that in nanocrystalline materials, the grain boundary movement through sliding is a distinct possibility as the dislocation activity becomes absent [46]. Hence, the mechanisms related to IHP in nano-QC regime appear to be very similar to that of nanocrystals through grain boundary sliding. It must be emphasized that this sliding is not like the creep mechanisms operating during high temperature deformation.

It is purely a shearing event at the grain boundaries which causes the softening effect in nano-QC or nanocrystalline materials. However, the mechanisms applicable for HP behavior of crystalline materials cannot be applicable for quasicrystalline materials since the dislocation activities at room temperature are negligible.

The strengthening observed in the HP regime of QC materials, however, does not appear to be high compared to the crystalline materials. This has been explained based on the fact that chemical ordering seems to be increasing during the initial stages of milling [40]. Thus it can be understood that the enhanced chemical ordering along with the reduction in grain size causes the localized shearing event (not the grain boundary shearing which is dominant in nanoscale) leading to shear band formation. It has been noted that even at finer grain sizes, shear band formation will encounter difficulties compared to coarse grains as the grain boundaries offer the resistance to the propagation of the shear bands.

However, if the grain size is well below a critical value, it appears that the shearing at grain boundaries is more predominant compared to that in the grain bodies. This is perhaps due to the increase of enough grain boundary area as well as boundary width. In view of the above, it is clear that the factors which cause the hindrance of the shearing event in grain sizes larger than the critical value need to be understood. The minor part of softening in IHP region can also be attributed to the chemical disordering (mainly due to phason disordering) of quasicrystals. However, the major part of softening is mainly due to the favorable thermally-activated-shearing along grain boundaries. The present analysis also suggests further study on the effect of grain boundary areas as well as chemical and phason disordering on the softening mechanisms of nanoquasicrystalline materials.

4. Conclusions

Nanoquasicrystalline phases produced by mechanical milling exhibit HP as well as IHP like behavior. However, in case of HP region, the dislocation pile-up phenomena are not responsible for the increase of hardness unlike metallic alloys. It is reasonable to speculate that the chemical ordering, which increases during the initial stages of milling along with the grain size reduction below the critical grain size appears to be responsible for creating hurdles for localized shearing for the formation of shear bands and consequent strengthening during HP regime. It requires further studies in this direction.

The critical grain size of 40 nm, below which IHP behavior was noted, has been found to be larger than that for normal metallic materials such as Cu, Ni, and Zn. The relative change of hardness in HP and IHP region is much less compared to nanocrystalline alloys. This can be attributed to the complexities of the structure and to the deformation mechanisms operating in the HP region, as the dislocation mediated process for quasicrystal is not at all possible at room temperature.

However, in the IHP regime, grain boundary sliding through shearing events, and not through creep mechanism similar to that in nanocrystalline materials, seems to be possible. Hence, it is understood that below the critical size, thermally activated shearing among atoms at grain boundaries becomes more dominant and accounts for the softening behavior leading to the IHP phenomena in nano-QC materials. The activation energy evaluated from this approach of grain boundary shearing, through thermally activated process, has been reported to be 82 kJ/mol and appears to be in reasonable agreement with the activation energy for grain boundary diffusion. However, it also requires further investigations to understand the micromechanisms of grain boundary shearing through high resolution electron microscopy.

Acknowledgments

N.K. Mukhopadhyay and V.C. Srivastava thankfully acknowledge the support of Alexander Humboldt Foundation (AvH) for pursuing the collaborative research work. F. Ali acknowledges the PIEAS for financial support. The support of ESRF through the experiment HD 482 is gratefully acknowledged.

References

[1] E.O. Hall, *Proc. Phys. Soc. (Lond.)***64**, 747 (1951).

[2] N.J. Petch, *J. Iron Steel Inst.* **174**, 25 (1953).

[3] R.W. Armstrong, *Yield, flow and fracture of polycrystals*, Ed. T.N. Baker, Applied Science Publishers, London 1983, p. 1.

[4] A. Lasalmonie, J.L. Strudel, *J. Mater. Sci.* **21**, 1837 (1986).

[5] N.K. Mukhopadhyay, P. Paufler, *Int. Mater. Rev.* **51**, 209 (2006).

[6] H.W. Song, S.R. Guo, Z.Q. Hu, *Nanostruct. Mater.* **11**, 203 (1999).

[7] C.C. Koch, J. Narayan, *Mater. Res. Soc. Symp. Proc.* **634**, B5.1.1 (2001).

[8] C. Suryanarayana, *Int. Mater. Rev.* **40**, 41 (1995).

[9] C. S. Pande, K.P. Cooper, *Prog. Mater. Sci.* **54**, 689 (2009).

[10] H. Chang, C.J. Altstetter, R.S. Averback, *J. Mater. Res.* **7**, 2962 (1992).

[11] U. Erb, *Nanostruct. Mater.* **6**, 533 (1995).

[12] J. Karch, R. Birringer, H. Gleiter, *Nature* **330**, 556 1987).

[13] S.Y. Chang, T.K. Chang, *J. Appl. Phys.* **101**, 033507 (2007).

[14] D. Jang, M. Atzmon, *J. Appl. Phys.* **93**, 9282 (2003).

[15] R.W. Siegel, *Mater. Sci. Forum* **235-238**, 851 (1997).

[16] C. Suryanarayana, D. Mukhopadhyay, S.N. Patankar, F.H. Froes, *J. Mater. Res.* **7**, 2114 (1992).

[17] F.A. Mohamed, *Metall. Mater. Trans.* **38A**, 340 (2007).

[18] C. Suryanarayana, *Mater. Today* **15**, 486 (2012).

[19] M.A. Meyers, A. Mishra, D.J. Benson, *Prog. Mater. Sci.* **51**, 427 (2006).

[20] H. Conrad, J. Narayan, *Scri. Mater.* **42**, 1025 (2000).

[21] H. Conrad, J. Narayan, *Appl. Phys. Lett.* **81**, 2241 (2002).

[22] H. Conrad, J. Narayan, *Acta Mater.* **50**, 5067 (2002).

[23] C. Suryanarayana, C.C. Koch, *Hyperfine Interact.* **130**, 5, (2000).

[24] H. Gleiter, *Prog. Mater. Sci.* **33**, 223 (1989).

[25] K.A. Padmanabhan, G.P. Dinda, H. Hahn, H. Gleiter, *Mater. Sci. & Eng. A* **452-453**, 462 (2007).

[26] P. P. Chattopadhyay, S.K. Pabi, I. Manna, *Z. Metallkd.* **91**, 1049 (2000).

[27] E.H. Saarivirta, *J. Alloys Comp.* **363**, 154-178 (2004).

[28] N.K. Mukhopadhyay, T.P. Yadav, *Isr. J. Chem.* **51**, 1185 (2011).

[29] C. Suryanarayana, *Mechanical Alloying and Milling*, Marcel Dekker, New York 2004.

[30] C. Suryanarayana, *Prog. Mater. Sci.* **46**, 1 (2001).

[31] M. Feuerbacher, C. Metzmacher, M. Wollgarten, K. Urban, B. Baufeld, M. Bartsch, U. Messerschmidt, *Mater. Sci. Engg A* **226-228**, 943 (1997).

[32] V. Azhazha, S. Dub, G. Khadzhay, B. Merisov, S. Malkin, A. Pugachov, *Philos. Mag.* **84**, 983 (2004).

[33] N.K. Mukhopadhyay, A. Belger, P. Paufler, P. Gille, *Philos. Mag.* **86,** 999 (2006).

[34] N.K. Mukhopadhyay, A. Belger, P. Paufler, E. Uhrig, S. Bruhne, W. Assmus, *J. Alloys & Comp.* **466**, 160 (2008).

[35] M. Abu Shaz, N.K. Mukhopadhyay, R.K. Mandal, O.N. Srivastava, *J. All. Comp.* **342**, 49 (2002).

[36] N.K. Mukhopadhyay, A. Belger, P. Paufler, D.H. Kim, *Mater. Sci. & Eng. A* **449-451**, 954 (2007).

[37] M. Reibold, A. Belger, N.K. Mukhopadhyay, P. Gille, P. Paufler, *Phys. Stat. Sol.* **202**, 2267 (2005).

[38] S.S. Kang, J.M. Dubois, *Europhys. Lett.* **18**, 45 (1992).

[39] S.H. Kim, K. Chattopadhyay, B.J. Inkson, G. Mobus, W.T. Kim, D.H. Kim, *J. Mater. Sci.* **41**, 6081 (2006).

[40] N.K. Mukhopadhyay, F. Ali, S. Scudino, M. Samadi Khoshkhoo, M. Stoica, V.C. Srivastava, V. Uhlenwinkel, G. Vaughan, C. Suryanarayana, J. Eckert, *Appl. Phys. Lett.* **103**, 201914 (2013).

[41] V.C Srivastava, V. Uhlenwinkel, A. Schultz, H.W. Zoch, N.K. Mukhopadhyay, S.G. Chowdhury, *Z. Kristallogr.* **223**, 211 (2008).

[42] N.K. Mukhopadhyay, F. Ali, V.C. Srivastava, T.P. Yadav, M. Sakaliyska, K.B. Surreddi, S. Scudino, V. Uhlenwinkel, J. Eckert, *Philos. Mag.* **91,** 2482 (2011).

[43] F. Ali, S. Scudino, S.M. Gorantla, V.C. Srivastava, H.R. Shahid, V. Uhlenwinkel, M. Stoica, G. Vaughan, N.K. Mukhopadhyay, J. Eckert, *Acta Mater.* **61**, 3819 (2013).

[44] N.K. Mukhopadhyay, S. Ranganathan, K. Chattopadhyay, *Philos. Mag. Lett.* **60**, 207 (1989).

[45] T.G. Nieh, J. Wadsworth, *Scr. Metall. Mater.* **25**, 955 (1991).

[46] J. Schiotz Jakob, F.D. Di Tolla, K.W. Jacobsen, *Nature* **39**, 561 (1998).